



SRC3 acetylates calmodulin in the mouse brain to regulate synaptic plasticity and fear learning

Received for publication, March 2, 2021, and in revised form, July 20, 2021. Published, Papers in Press, August 4, 2021.
<https://doi.org/10.1016/j.jbc.2021.101044>

Hai-Long Zhang^{1,2,†}, Wei Han^{1,†}, Yin-Quan Du^{1,†}, Bing Zhao¹, Pin Yang¹, and Dong-Min Yin^{1,*}

From the ¹Key Laboratory of Brain Functional Genomics, Ministry of Education and Shanghai, School of Life Science, East China Normal University, Shanghai, China and ²Jiangsu Key Laboratory of Neuropsychiatric Diseases and Institute of Neuroscience, Soochow University, Suzhou, China

Edited by Roger Colbran

Protein acetylation is a reversible posttranslational modification, which is regulated by lysine acetyltransferase (KAT) and lysine deacetyltransferase (KDAC). Although protein acetylation has been shown to regulate synaptic plasticity, this was mainly for histone protein acetylation. The function and regulation of nonhistone protein acetylation in synaptic plasticity and learning remain largely unknown. Calmodulin (CaM), a ubiquitous Ca²⁺ sensor, plays critical roles in synaptic plasticity such as long-term potentiation (LTP). During LTP induction, activation of NMDA receptor triggers Ca²⁺ influx, and the Ca²⁺ binds with CaM and activates calcium/calmodulin-dependent protein kinase II α (CaMKII α). In our previous study, we demonstrated that acetylation of CaM was important for synaptic plasticity and fear learning in mice. However, the KAT responsible for CaM acetylation is currently unknown. Here, following an HEK293 cell-based screen of candidate KATs, steroid receptor coactivator 3 (SRC3) is identified as the most active KAT for CaM. We further demonstrate that SRC3 interacts with and acetylates CaM in a Ca²⁺ and NMDA receptor-dependent manner. We also show that pharmacological inhibition or genetic downregulation of SRC3 impairs CaM acetylation, synaptic plasticity, and contextual fear learning in mice. Moreover, the effects of SRC3 inhibition on synaptic plasticity and fear learning could be rescued by 3KQ-CaM, a mutant form of CaM, which mimics acetylation. Together, these observations demonstrate that SRC3 acetylates CaM and regulates synaptic plasticity and learning in mice.

Synaptic plasticity is crucial for several brain functions such as learning and memory. It is regulated by long-term mechanisms such as gene transcription (1, 2), as well as acute mechanisms at synapses including protein phosphorylation (3, 4). Protein acetylation is regulated by lysine acetyltransferase (KAT) and lysine deacetylase (KDAC) and was discovered initially as a posttranslational modification of histone proteins to activate gene transcription (5). While protein acetylation has been implicated in synaptic plasticity

and learning before, this was mainly for histone protein acetylation (6–9).

Calmodulin (CaM), a ubiquitous Ca²⁺ sensor, plays critical roles in Ca²⁺ signaling and synaptic plasticity (10–14). In an accompanying paper in this issue, we revealed acetylation of CaM on three lysine residues (K22, 95, and 116), which are conserved across species (15). Moreover, CaM acetylation could be upregulated by neural activities, which play important roles in synaptic plasticity and learning (15). However, the KAT responsible for CaM acetylation and how acetylation of CaM is regulated by neural activities remain largely unknown.

There are 20 total KAT proteins, which can be classified into four major families (16). Most if not all KAT proteins are expressed in the nucleus to regulate gene transcription (9). In addition, some KAT proteins are expressed in the cytoplasm and can shuttle between the nucleus and cytoplasm (17). In this study, we performed unbiased screen to identify steroid receptor coactivator 3 (SRC3) as the KAT that interacts with and acetylates CaM in a Ca²⁺-dependent manner. In agreement, neural activities increase the interaction between SRC3 and CaM in an NMDA receptor-dependent way. Lastly, we demonstrate that SRC3 regulates synaptic plasticity and contextual fear learning at least partially through CaM acetylation. Together, these observations provide evidence for a role of SRC3-mediated CaM acetylation in regulating synaptic plasticity and learning.

Results

Increase of CaM acetylation by SRC3 overexpression in HEK293 cells

Since CaM acetylation is important for synaptic plasticity and learning (15), we aim to identify the KAT that can acetylate CaM. The KAT proteins are generally classified into four major families (Fig. 1A) (16). Given that CaM is highly expressed in the cytoplasm and synaptosomes (including both pre and postsynaptic fractions), we reason that the KAT responsible for CaM acetylation is relatively enriched in the cytoplasm or synaptosomes, instead of or in addition to the nucleus. To investigate the subcellular distribution of KAT, we separated mouse brain tissues into nuclear (N), cytosolic (C), and crude synaptosome (P2)

[†] These authors contributed equally to this work.

* For correspondence: Dong-Min Yin, dmyin@brain.ecnu.edu.cn.

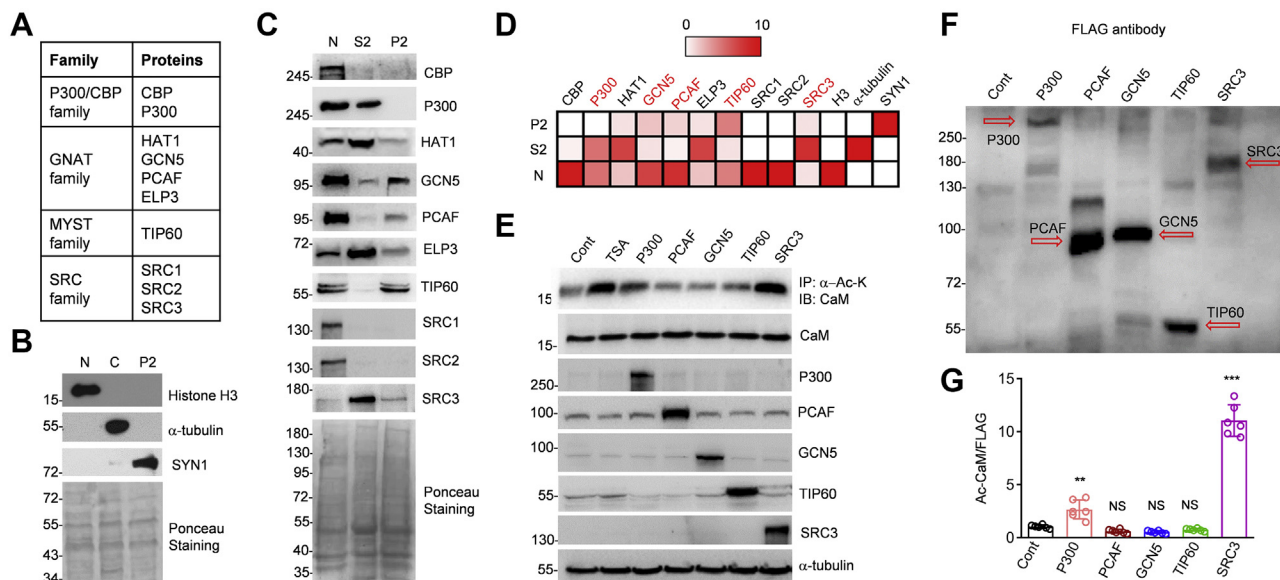


Figure 1. Subcellular distribution of KAT proteins and acetylation of CaM by SRC3 in HEK293 cells. *A*, the family and representative proteins of KAT. *B*, expression of Histone H3 (H3), α -tubulin, and synapsin 1 (SYN1) in the nuclear (N), cytoplasmic (S2), and P2 fractions. The *bottom image* is the Ponceau staining. *C*, distribution of different KAT proteins in the nuclear (N), cytoplasmic (S2) and P2 fraction of mouse forebrain. Histone H3 (H3), α -tubulin, and Synapsin1 (SYN1) are markers for the N, S2, and P2 fractions. *D*, heat map of KAT protein levels in the nuclear (N), cytoplasmic (S2), and P2 fractions of mouse forebrain. Original western blots were shown in *panel C*. *E*, overexpression of SRC3 induces acetylation of CaM in HEK293 cells. The total lysates from HEK293 cells treated with 1 μ M TSA or transfected with different KAT plasmids for 36 h were probed with the indicated Abs. *F*, expression of Flag-tagged KAT constructs in HEK 293 cells. The total lysates of HEK293 cells transfected with different Flag-tagged KAT constructs were probed with anti-Flag antibodies. The *arrows* indicate the main bands for different KAT proteins. *G*, SRC3 has a higher capacity to acetylate CaM than other KATs. Shown were acetylated CaM levels normalized by the intensity of Flag signal verified in *panel F*. Data were represented as mean \pm SD. NS, not significant, $**p = 0.0024$, $***p < 0.0001$, compared with control, one-way ANOVA, $n = 6$, data were normalized by control.

fractions (Fig. 1B). The purity of the N, C and P2 fractions was confirmed by the enrichment of different markers: histone protein H3 in the N, α -tubulin in the C and Synapsin 1 in the P2 (Fig. 1B). All the KATs we examined were expressed in the nucleus (Fig. 1C). For the P300/CBP family, P300 is expressed in the cytoplasm in addition to the nucleus (Fig. 1, C and D). Among the GNAT family proteins, GCN5 and PCAF were relatively higher in the P2, compared with HAT1 and ELP3 (Fig. 1, C and D). TIP 60 is expressed in both the nucleus and P2 (Fig. 1, C and D). In the SRC family, SRC3 rather than SRC1 or SRC2 is highly expressed in the cytoplasm (Fig. 1, C and D).

Due to these findings, we focused on the following proteins in each KAT family: P300 for the P300/CBP family; PCAF and GCN5 for the GNAT family; TIP60 for the MYST family; SRC3 for the SRC family (Fig. 1D). To determine which KAT can acetylate CaM, we overexpressed the candidate KATs in HEK293 cells and 36 h after transfection of the plasmids, acetylated proteins were precipitated with anti-Ac-K antibody and probed by anti-CaM antibody. As a positive control, treatment with TSA, a pan KDAC inhibitor (18), for 30 min could induce CaM acetylation in HEK293 cells (Fig. 1E). Intriguingly, expression of SRC3 and P300 rather than other KATs led to CaM acetylation in HEK293 cells (Fig. 1E). Flag immunoblotting indicated that the expression levels of SRC3 were similar with P300 and TIP60, but lower than PCAF and GCN5 (Fig. 1F). The acetylated CaM levels normalized by the intensity of Flag signal verified that SRC3 had a higher capacity to acetylate CaM than other KATs (Fig. 1G). Altogether, these

results demonstrate that overexpression of SRC3 can increase CaM acetylation in HEK293 cells.

SRC3 acetylates CaM in a calcium-dependent way

SRC3 (also known as p/CIP, RAC3, AIB1, ACTR, TRAM1, and NCOA3) is a member of the family of steroid receptor coactivators and has been implicated in regulating steroid hormone signaling (19). To investigate whether SRC3 could acetylate CaM, recombinant GST-CaM proteins were subjected to *in vitro* acetylation assay by incubation with Flag-SRC3 purified from HEK293 cells. The resulting GST-CaM proteins after *in vitro* acetylation assay were probed with anti-Ac-K antibodies. GST-CaM purified from bacteria could not be acetylated without SRC3 (Fig. 2A). However, Flag-SRC3 could acetylate GST-CaM *in vitro* (Fig. 2A). Analysis of previous proteomic studies and publicly available database revealed that CaM could be acetylated on three lysine residues (K 22, 95, and 116) in mouse brain (15). SRC3-mediated acetylation of CaM was abolished by the 3KR mutation (Fig. 2, A and B). By contrast, SRC3 was able to interact with 3KR-CaM (Fig. 2, A and C).

To investigate whether SRC3 could acetylate CaM on the three lysine residues—K22, 95, and 116, the GST-CaM proteins after *in vitro* acetylation assay were probed with site-specific anti-Ac-CaM antibodies (15). The anti-Ac-K22-CaM antibody could detect the acetylation of WT, K95R, and K116R-CaM but not K22R-CaM and vice versa (Fig. 2D). These results demonstrate that SRC3 can acetylate CaM on

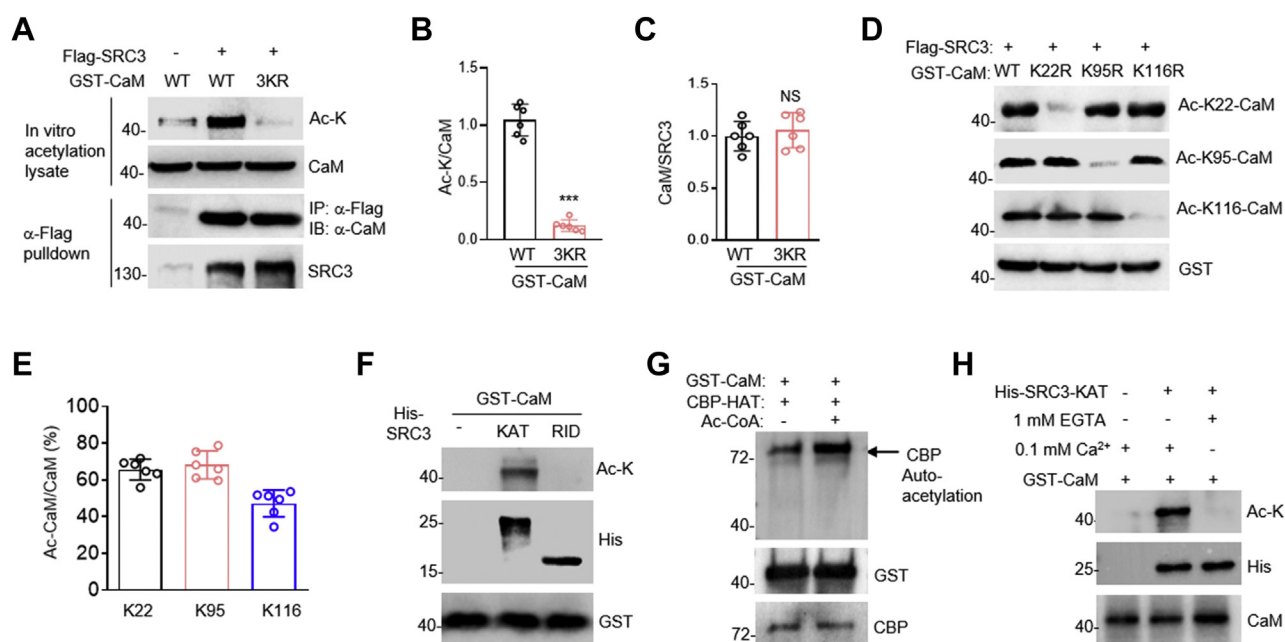


Figure 2. Acetylation of CaM by SRC3 in a calcium-dependent manner. *A*, Flag-SRC3 purified from HEK293 cells could acetylate GST-WT-CaM. 3KR mutation diminished CaM acetylation, but not SRC3-CaM interaction. Flag-SRC3 was immunoprecipitated by anti-Flag-conjugated beads and then incubated with GST-tagged WT or 3KR-CaM for *in vitro* acetylation assay (top two lanes). In another experiment, Flag-SRC3 was immunoprecipitated by anti-Flag-conjugated beads and then incubated with GST-tagged WT or 3KR-CaM for pull-down assay (bottom two lanes). *B*, quantification of Ac-K/CaM in panel *A*. Data were represented as mean \pm SD. *** $p < 0.0001$, *t* test, $n = 6$, data were normalized to WT-CaM. *C*, quantification of CaM-SRC3 interaction as CaM/SRC3 in panel *A*. Data were represented as mean \pm SD. NS, not significant, *t* test, $n = 6$, data were normalized to WT-CaM. *D*, CaM acetylation at K22, 95, and 116 by SRC3. GST-CaM was subjected to *in vitro* acetylation assay with Flag-SRC3 purified from HEK293 cells overexpressing Flag-SRC3, and the reaction was probed with site-specific anti-CaM antibodies. Note that the site-specific antibodies against Ac-CaM cannot recognize the CaM proteins with the K-R mutation. *E*, Stoichiometry levels of K22, 95, and 116 acetylated by SRC3 *in vitro* from panel *D*. Data were represented as mean \pm SD. $n = 6$. *F*, the KAT domain instead of RID of SRC3 could acetylate CaM. His-tagged SRC3 HAT domain and RID were purified from bacteria and used for *in vitro* acetylation assay with GST-CaM. *G*, purified CBP KAT domain cannot acetylate GST-CaM. *H*, acetylation of CaM by the KAT domain of SRC3 is Ca^{2+} -dependent. All proteins were purified from bacteria. Acetylation was performed in the presence of 0.1 mM Ca^{2+} or 1 mM EGTA.

K22, K95, and K116. The stoichiometry analysis indicated that SRC3 could acetylate 66% K22, 68% K95, and 47% K116 *in vitro* (Fig. 2E). SRC3 has an RID (receptor-interaction domain) and a KAT domain (19). We generated recombinant His-tagged RID and KAT domain of SRC3 and incubated them with GST-CaM. Our data indicate that CaM is acetylated by the KAT, but not the RID domain of SRC3 (Fig. 2F). By contrast, CaM could not be acetylated by the KAT domain of CBP (Fig. 2G), indicating the specificity of SRC3 in regulating CaM acetylation. Moreover, the KAT domain can acetylate GST-CaM in the presence of Ca^{2+} but not in the presence of EGTA (Fig. 2H). These results demonstrate that SRC3 acetylates CaM in a Ca^{2+} -dependent manner.

SRC3 interacts with CaM in a calcium-dependent manner

In the following study, we investigate whether SRC3 could interact with CaM. To this end, we performed GST pull-down assay using purified His-tagged SRC3-KAT domain and GST-CaM proteins. His-SRC3-HAT domain could bind with CaM under 0.01 mM Ca^{2+} (Fig. 3A). Moreover, this interaction was enhanced in the presence of 0.1 mM Ca^{2+} and was abolished with 1 mM EGTA (Fig. 3, A and B). These results suggest that SRC3-CaM interaction was direct and required Ca^{2+} . The K_d value of Ca^{2+} for the interaction between GST-CaM and His-SRC3-KAT is 2.734 μM (Fig. 3C). To further study whether

SRC3 could interact with CaM in mammalian cells, we overexpressed Flag-SRC3 in HEK293 cells. The cell lysates were immunoprecipitated with anti-Flag antibodies and probed with anti-CaM antibodies. As shown in Figure 3D, CaM was coimmunoprecipitated (Co-IP) with SRC3 when the Co-IP buffer did not contain EGTA. However, the co-IP disappeared when the incubation buffer contains 1 mM EGTA (Fig. 3D). These data imply that SRC3 interacts with CaM in mammalian cells in a Ca^{2+} -dependent way. Next, we address whether neural activity could enhance SRC3-CaM interaction. Toward this aim, we performed chemical LTP (cLTP) stimulation in hippocampal slices for 10 min, and after that, we collected the total lysates for Co-IP experiments. Intriguingly, cLTP stimulation increased the interaction between SRC3 and CaM, and the potentiation could be blocked by the NMDAR antagonist AP5 (Fig. 3, E and F). Together, these results demonstrate that the SRC3 interacts with CaM in a way dependent on Ca^{2+} and NMDAR.

Inhibition of SRC3 impairs CaM acetylation and hippocampal LTP

SRC3 is highly expressed in hippocampal pyramidal neurons revealed by *Src3* reporter mice (20). cLTP stimulation could increase CaM acetylation and activate CaMKII α in hippocampal slices (Fig. 4A). Autophosphorylated CaMKII α was

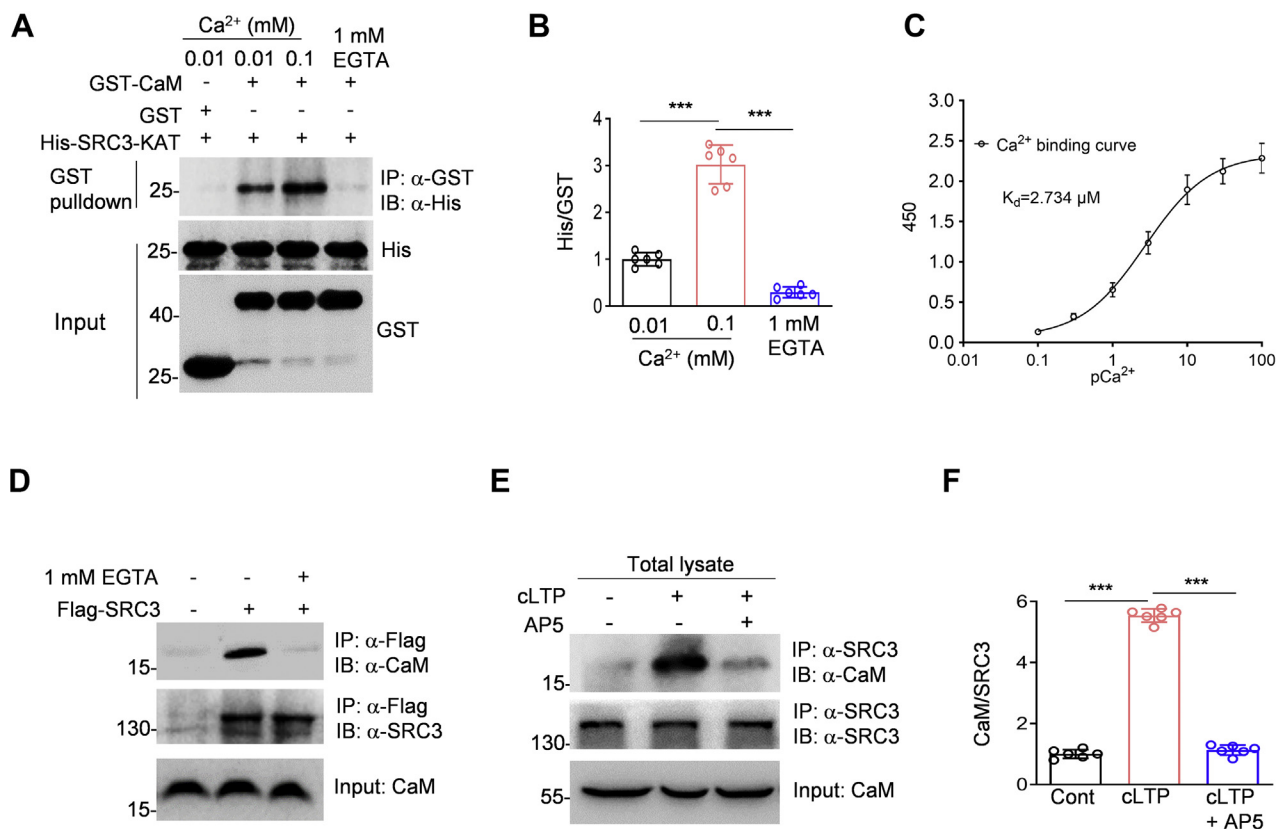


Figure 3. CaM-SRC3 interaction in a Ca²⁺ and NMDAR-dependent manner. *A*, increased CaM-SRC3 interaction by Ca²⁺. His-SRC3-KAT and GST-CaM were purified from bacteria and their interaction was investigated by GST pull-down during which acetylation could not occur. *B*, quantification of CaM-SRC3 interaction as His/GST in panel *A*. Data were represented as mean ± SD. ****p* < 0.0001, one-way ANOVA, *n* = 6, data were normalized to 0.01 mM Ca²⁺. *C*, the binding curve of GST-CaM and His-SRC3-KAT under different Ca²⁺ concentrations. The K_d of Ca²⁺ for the interaction between GST-CaM and His-SRC3-KAT is 2.734 μM, *n* = 3. Data were represented as mean ± SD. *D*, CaM-SRC3 interaction in HEK293 cells depends on Ca²⁺. The immunoprecipitation (IP) of Flag-SRC3 was probed with anti-CaM antibodies. The CaM-SRC3 interaction was abolished when the IP buffer contained 1 mM EGTA. *E*, increased CaM-SRC3 interaction by cLTP, which is dependent on NMDAR. The CaM-SRC3 interaction was assessed by coimmunoprecipitation (co-IP) from total lysate of hippocampal slices with different treatment. The co-IP was performed in RIPA buffer without EGTA or detergent. *F*, quantification of CaM-SRC3 interaction as CaM/SRC3 in panel *E*. Data were represented as mean ± SD. ****p* < 0.0001, one-way ANOVA, *n* = 6, data were normalized to control.

detected with a phospho-specific antibody against Thr²⁸⁶, whose phosphorylation is an indicator of CaMKIIα activation (21). To determine whether SRC3 is important for CaM acetylation and CaMKIIα activation after cLTP stimulation, the hippocampal slices were treated with 1 μM SI-2, an SRC3 inhibitor (22), for 20 min before cLTP stimulation. As shown in Figure 4, A–C, cLTP-induced CaM acetylation and CaMKIIα activation in hippocampal slices were reduced by SI-2. CaMKIIα could phosphorylate the AMPA receptor subunit GluR1 at Ser⁸³¹ during LTP (23, 24). Consistent with the reduction of CaMKIIα activity after cLTP stimulation in the presence of SI-2, p-GluR1 Ser⁸³¹ also decreased after treatment with SI-2 (Fig. 4, A and D). These results indicate that SRC3 inhibition impairs CaM acetylation and CaMKIIα activation by cLTP stimulation.

To investigate whether SRC3 could regulate functional LTP, we applied theta burst stimulation (TBS) into hippocampal slices to induce LTP at SC-CA1 synapses (Fig. 4E) (21). Hippocampal slices were treated with SI-2, an SRC3 inhibitor for 20 min before TBS, which effectively attenuated posttetanic potentiation (PTP) and LTP in a dose-dependent manner (Fig. 4, F–H). Treatment of hippocampal slices with 1 μM SI-2

for 20 min did not affect the input–output (I/O) curves or paired-pulse facilitation (PPF) of SC-CA1 synapses (Fig. 4, I and J), indicating no effects on basal glutamatergic transmission by acute SRC3 inhibition. Treatment of hippocampal slices with 1 μM SI-2 10 min after TBS for 20 min had no effect on PTP or LTP (Fig. 4, K–M). These results demonstrate that SRC3 is important for LTP induction but not maintenance.

SRC3 regulates hippocampal LTP through acetylation of CaM

Next, we determine whether SRC3 regulation of LTP is mediated by CaM acetylation. To this end, we performed whole-cell LTP recording in CA1 pyramidal neurons and observed the effects of purified GST-WT-CaM and GST-3KQ-CaM proteins (acetylation mimicking CaM) (15) that were delivered into CA1 pyramidal neurons *via* the recording pipettes (Fig. 5A). Acute treatment with SI-2 did not affect the basic properties of CA1 pyramidal neurons such as input resistance (Fig. 5B). However, high-frequency stimulation (HFS)-induced PTP and LTP in CA1 pyramidal neurons were reduced by acute treatment with SI-2 when the neurons were

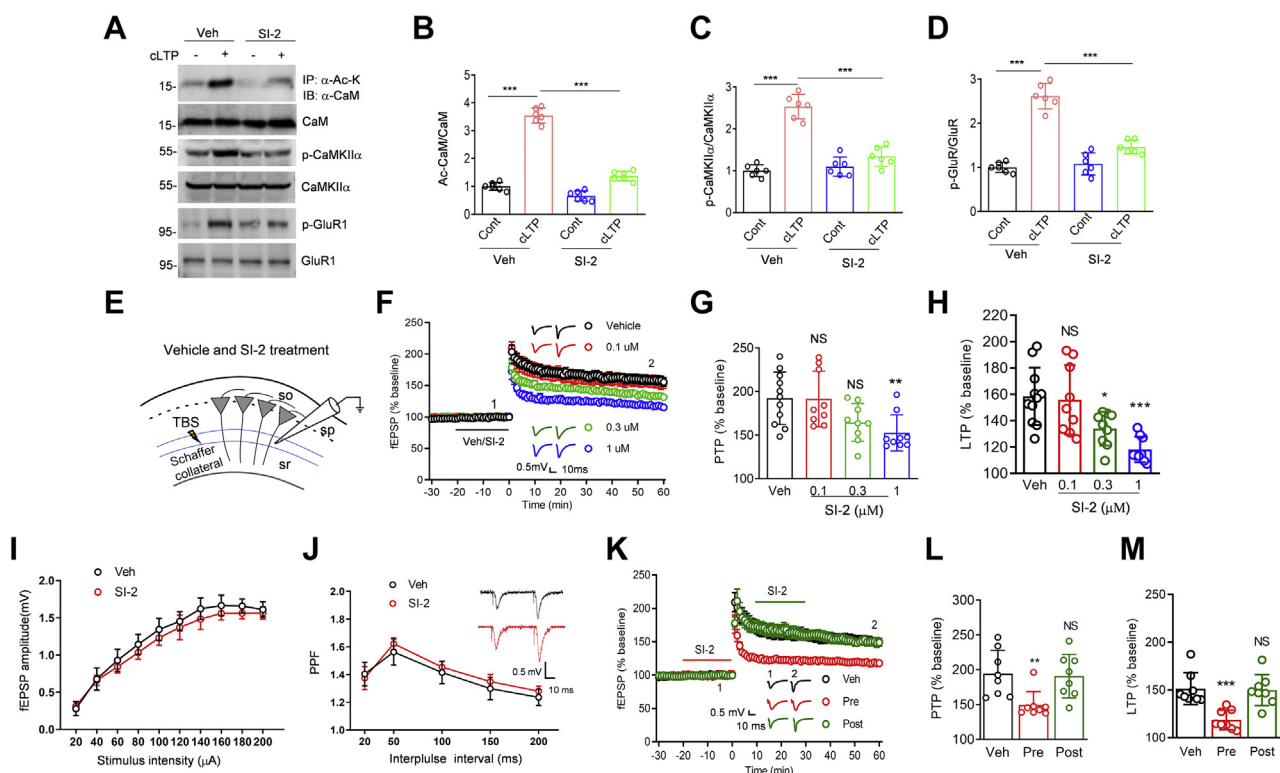


Figure 4. Impaired CaM acetylation and hippocampal LTP by SRC3 inhibition. *A*, increased Ac-CaM, p-CaMKII α , and p-GluR1 after cLTP stimulation were attenuated by 1 μ M Si-2. Total lysate of hippocampal slices after different treatment was probed for Ac-CaM, CaM, p-CaMKII α , CaMKII α , p-GluR1, and GluR1. *B–D*, quantification of Ac-CaM/CaM (*B*), p-CaMKII α /CaMKII α (*C*), and p-GluR1/GluR1 (*D*) in panel *A*. Data were represented as mean \pm SD. *** p < 0.0001, two-way ANOVA followed by Tukey's multiple comparisons test, n = 6, data were normalized to control. *E*, diagram showing field EPSP recording at SC-CA1 synapses. WT hippocampal slices were treated with vehicle or Si-2. *F*, normalized fEPSP amplitudes were plotted every 1 min for hippocampal slices treated with vehicle or different concentrations (0.1, 0.3, 1 μ M) of Si-2, which was applied during the period indicated by the bar. *G* and *H*, Si-2 attenuated PTP (*G*) and LTP (*H*) in a dose-dependent manner. Data in panel *F* were quantified. Data were represented as mean \pm SD. NS, not significant, * p = 0.0187, ** p = 0.0062, *** p = 0.001, compared with Veh, one-way ANOVA, n = 11 slices from five mice for Veh, n = 9 slices from four mice for other groups. Veh: vehicle. *I*, Si-2 (1 μ M) did not alter input–output (*I/O*) curves at SC-CA1 synapses. Data were represented as mean \pm SD. *F* (1,16) = 3.736, p = 0.0711, two-way-ANOVA, n = 9 slices from four mice for each group. *J*, Si-2 (1 μ M) did not affect paired pulse facilitation (PPF) at SC-CA1 synapses. Data were represented as mean \pm SD. *F* (1,22) = 1.975, p = 0.1738, two-way-ANOVA, n = 12 slices from four mice for each group. *K*, normalized fEPSP amplitudes were plotted every 1 min for hippocampal slices treated with vehicle or 1 μ M Si-2, which was applied during the period indicated by the bar. *L* and *M*, Si-2 (1 μ M) inhibited LTP induction but not maintenance. Data of PTP (*L*) and LTP (*M*) in panel *K* were quantified. Data were represented as mean \pm SD. NS, not significant, ** p = 0.0093, *** p = 0.0004, compared with Veh, one-way ANOVA, n = 8 slices from four mice for each group. Veh: vehicle, Pre: before TBS, Post: after TBS.

delivered with GST-WT-CaM proteins (Fig. 5, C–E). Intriguingly, these inhibitory effects were diminished in neurons delivered with GST-3KQ-CaM proteins (Fig. 5, C–E). The rescue effects by acetylation-mimicking CaM suggest that CaM acetylation is downstream of SRC3, contributing to LTP.

Downregulation of SRC3 attenuates CaM acetylation and hippocampal LTP

To verify that SRC3 in adult hippocampus is important for CaM acetylation and LTP with a genetic approach, we took use of the CRISPR-Cas9 technique (22). To this end, we injected

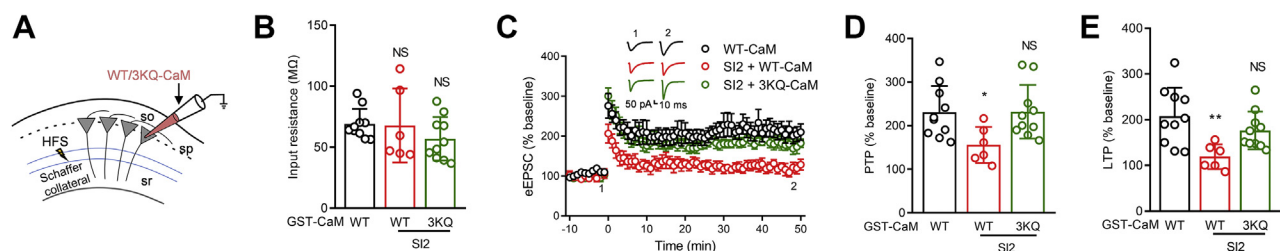


Figure 5. SRC3 regulates hippocampal LTP through acetylation of CaM. *A*, diagram showing whole-cell recording of eEPSC in CA1 pyramidal neurons of mouse hippocampus. Recording pipettes were infused with GST-tagged WT or 3KQ-CaM proteins. *B*, the input resistance of CA1 pyramidal neurons was not affected by Si-2 (1 μ M) treatment. Data were represented as mean \pm SD. NS, not significant, compared with WT-CaM, one-way ANOVA, n = 10 cells from ten mice for WT-CaM and Si-2 + 3KQ-CaM, n = 6 cells from six mice for Si-2 + WT-CaM. *C*, normalized eEPSC amplitudes were plotted every 1 min for CA1 pyramidal neurons infused with 100 nM GST-WT-CaM or GST-3KQ-CaM proteins with or without Si-2 treatment. *D* and *E*, 3KQ-CaM rescued the deficit of PTP (*D*) and LTP (*E*) after SRC3 inhibition. Data in panel *C* were quantified. Data were represented as mean \pm SD. NS, not significant, * p = 0.0346, ** p = 0.0036, compared with GST-WT-CaM, one-way ANOVA, n = 10 cells from ten mice for WT-CaM and Si-2 + 3KQ-CaM, n = 6 cells from six mice for Si-2 + WT-CaM.

adenoassociated virus (AAV) expressing *Src3* or control gRNA and EGFP into the hippocampal CA1 region of adult Rosa26-Cas9 knockin mouse (Fig. 6, A–C). Three weeks after injection, *Src3* gRNA efficiently reduced the protein levels of SRC3, but not SRC1 or SRC2 (Fig. 6, D and E). The CaM acetylation and CaMKII α activation after cLTP stimulation were significantly reduced in SRC3 knockdown (SRC3 KD) slices, compared with control slices (Fig. 6, F–H). These results suggest that downregulation of SRC3 in adult hippocampus is sufficient to impair CaM acetylation and CaMKII α activation after cLTP stimulation. We next performed LTP recording at SC-CA1 synapses in hippocampal slices 3 weeks after AAV injection (Fig. 6I). The *Src3* gRNA severely impaired TBS-induced PTP and LTP, compared with control gRNA (Fig. 6, J–L), demonstrating that SRC3 in adult hippocampus is important for LTP. Together with the results with SRC3 inhibitor SI-2, these results demonstrate the importance of SRC3 in regulating CaM acetylation and hippocampal LTP.

Importance of SRC3 in contextual fear learning

The LTP at SC-CA1 synapses in the hippocampus is coupled to contextual fear learning (25, 26). Next, we address whether SRC3 is important for contextual fear learning. Toward this aim, we injected the SRC3 inhibitor SI-2 or vehicle into the lateral ventricles of adult mouse brain. Consistent with our previous finding, pairing with unconditioned stimulation (US) and conditioned stimulation (CS) during fear conditioning increased CaM acetylation (Fig. 7A). However, the elevation of CaM acetylation, p-CaMKII α , and p-GluR1 after pairing with US and CS was greatly attenuated by the SRC3 inhibitor SI-2 (Fig. 7, A–D), which suggests a role of SRC3 in CaM acetylation and CaMKII α activation during fear conditioning.

Strikingly, SI-2 injection 1 h before pairing of US and CS severely impaired contextual fear memory (Fig. 7E). By contrast, fear memory was not altered by SI-2 delivery 1 h

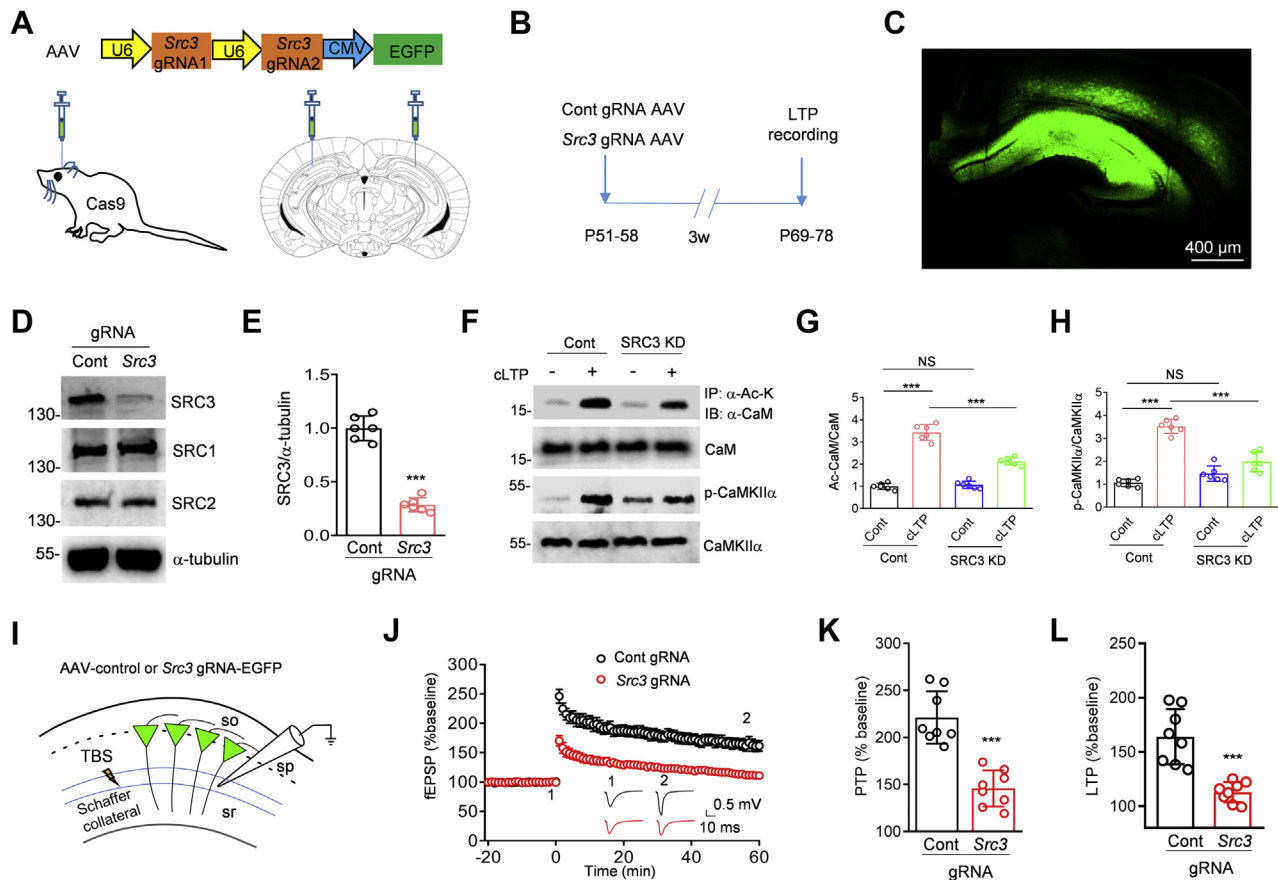


Figure 6. Attenuated CaM acetylation and hippocampal LTP by SRC3 downregulation. A, top, schematic diagram of AAV-*Src3* gRNA-EGFP. U6, human U6 Polymerase III promoter, CMV, human cytomegalovirus promoter, bottom, diagram showing the stereotaxic injection of AAV-*Src3* gRNA-EGFP into the hippocampus of Rosa26-Cas9 knockin mice. B, experimental design. C, expression of EGFP in the hippocampus 3 weeks after AAV injection. Scale bar, 400 μ m. D, reduced protein levels of SRC3 in Rosa26-Cas9 hippocampus injected with *Src3* gRNA AAV. The hippocampal lysates were probed with the indicated Abs. E, quantification of SRC3/ α -tubulin in panel D. Data were represented as mean \pm SD. *** p < 0.0001, t test, n = 6, data were normalized to control gRNA. F, increased Ac-CaM, p-CaMKII α after cLTP stimulation were attenuated by SRC3 knockdown (KD). Total lysate of hippocampal slices after different treatment were probed for Ac-CaM, CaM, p-CaMKII α , and CaMKII α . G and H, quantification of Ac-CaM/CaM (G) and p-CaMKII α /CaMKII α (H) in panel F. Data were represented as mean \pm SD. NS, not significant, *** p < 0.0001, two-way ANOVA followed by Tukey's multiple comparisons test, n = 6, data were normalized to control. I, diagram showing field EPSP recording at SC-CA1 synapses. Rosa26-Cas9 mice were injected with AAV expressing control or *Src3* gRNA and EGFP. J, normalized fEPSP amplitudes were plotted every 1 min for Rosa26-Cas9 hippocampal slices injected with indicated AAV. K and L, reduced PTP (K) and LTP (L) in mice injected with *Src3* gRNA AAV. Data in panel J were quantified. Data were represented as mean \pm SD. *** p < 0.0001, t test, n = 8 slices from four mice for each group.

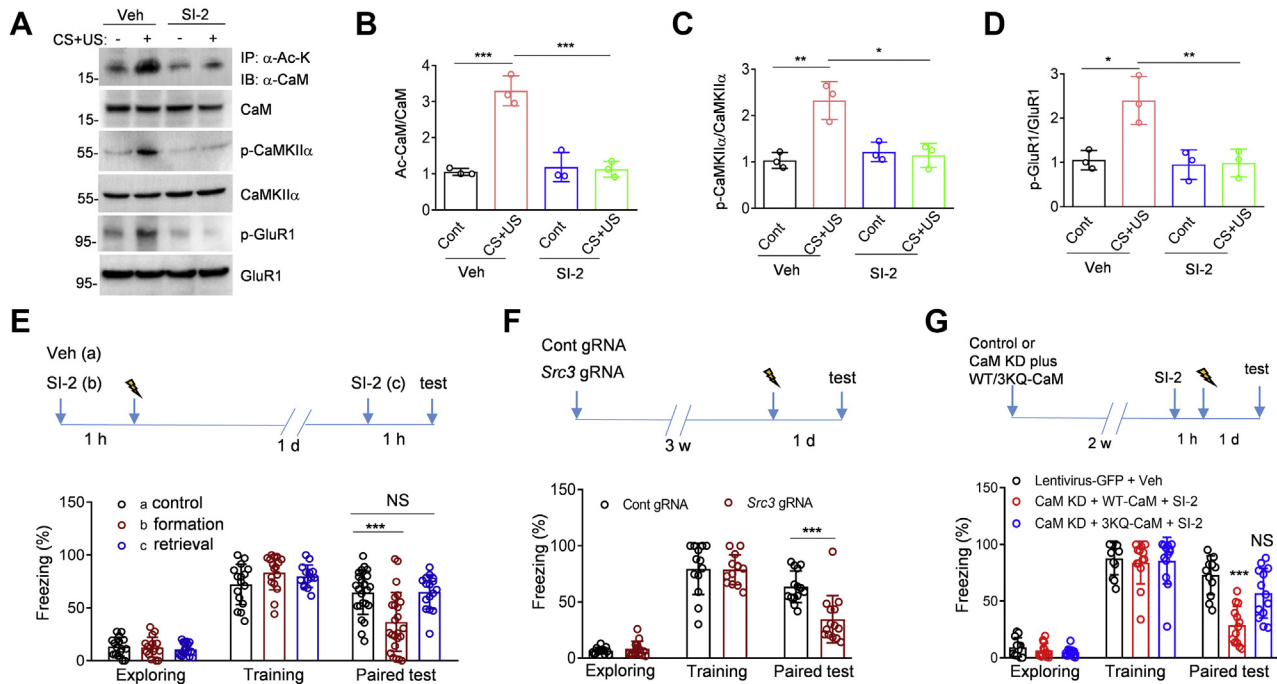


Figure 7. Importance of SRC3 in contextual fear learning. A, increased Ac-CaM, p-CaMKII α , and p-GluR1 after contextual fear conditioning were attenuated by SI-2. Total lysates of hippocampus from different groups of mice were probed for Ac-CaM, CaM, p-CaMKII α , CaMKII α , p-GluR1, and GluR1. B–D, quantification of Ac-CaM/CaM (B), p-CaMKII α /CaMKII α (C), and p-GluR1/GluR1 (D) in panel A. Data were represented as mean \pm SD. *** p = 0.0003 for column A and B, *** p = 0.0005 for column B and D in panel B, ** p = 0.0085, * p = 0.013 in panel C, * p = 0.0118, ** p = 0.0094 in panel D, two-way ANOVA followed by Tukey's multiple comparisons test, n = 3, data were normalized to control. E, reduced freezing during paired tests by SI-2 treatment 1 h before training. SI-2 had no effect on freezing when it was delivered 1 h before paired tests. Data were represented as mean \pm SD. NS, not significant, *** p = 0.0007, two-way ANOVA followed by Dunnett's multiple comparisons test, n = 16 for group a (control), n = 16 for group b (formation), n = 12 for group c (retrieval). Top, schematic diagram of behavioral tests. F, reduced freezing during paired tests in Rosa26-Cas9 mice injected with AAV expressing *Src3* gRNA. Data were represented as mean \pm SD. *** p = 0.0008, two-way ANOVA followed by Sidak's multiple comparisons test, n = 14 for each group. Top, schematic diagram of behavioral tests. G, 3KQ-CaM partially rescued fear learning deficits by SI-2. The mice receiving lentivirus expressing CaMKD+WT-CaM or CaMKD+3KQ-CaM were treated with SI-2 1 h before training. Data were represented as mean \pm SD. NS, not significant, *** p < 0.0001, two-way ANOVA followed by Dunnett's multiple comparisons test, compared with control, n = 13 for each group. Top, schematic diagram of behavioral tests.

before the paired test (Fig. 7E). These results suggest that SRC3 may be important for fear learning but not fear memory retrieval. Similar effects were observed in mice where SRC3 proteins were downregulated in adult hippocampus using CRISPR/Cas9 technique (Fig. 7F). These results indicate the importance of SRC3 in contextual fear learning. Notice that neither inhibition nor downregulation of SRC3 in adult mice affected locomotion in the open field (Fig. 8).

Lastly, we determine whether SRC3 regulation of fear learning is mediated by CaM acetylation. To this end, we did stereotaxic injection of lentivirus expressing *Cam* shRNA plus shRNA-resistant WT-CaM (CaMKD+WT) or CaMKD+3KQ-CaM (acetylation-mimicking CaM) (15) into CA1 hippocampus region. Two weeks after lentivirus injection, the mice were subjected to contextual fear conditioning (Fig. 7G). Fear learning was reduced by the SRC3 inhibitor SI-2 in mice

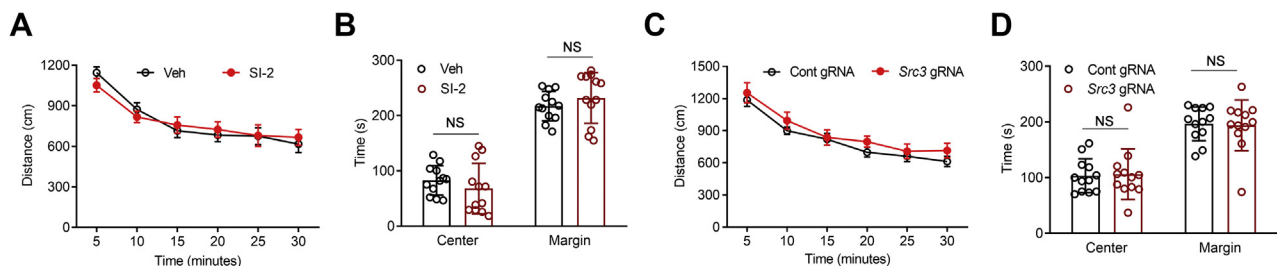


Figure 8. No effects of SRC3 inhibition or downregulation on locomotion. A, equal distance traveled during the first 30 min in open field for mice treated with vehicle or SI-2. Data were represented as mean \pm SD. Genotype F (1,22) = 0.3879, p = 0.5398, two-way ANOVA, n = 12 for each group. B, similar time staying in the center and margin of the open field during the first 5 min for mice treated with vehicle or SI-2. Data were represented as mean \pm SD. NS, not significant, p = 0.5613, two-way ANOVA followed by Sidak's multiple comparisons test, n = 12 for each group. C, equal distance traveled during the first 30 min in open field for Rosa26-Cas9 mice receiving hippocampal injection of the indicated AAV. Data were represented as mean \pm SD. NS, not significant, Genotype F (1,22) = 0.9887, p = 0.3309, two-way ANOVA, n = 12 for each group. D, similar time staying in the center and margin of the open field during the first 5 min for Rosa26-Cas9 mice receiving hippocampal injection of the indicated AAV. Data were represented as mean \pm SD. NS, not significant, p = 0.9811, two-way ANOVA followed by Sidak's multiple comparisons test, n = 12 for each group.

expressing CaMKD+WT-CaM (Fig. 7G). However, this inhibitory effect was diminished in mice expressing CaMKD+3KQ-CaM (Fig. 7G). The rescue effect by acetylation-mimicking CaM suggests that CaM acetylation is downstream of SRC3, contributing to contextual fear learning.

Discussion

In this study, we identified SRC3 as the KAT that interacts with and acetylates CaM. CaM could be acetylated by SRC3 purified from HEK293 cells. Moreover, acetylation was detectable when CaM was incubated with recombinant KAT domain of SRC3, but not that of CBP. These results suggest that CaM is a direct substrate of SRC3. CaM acetylation by SRC3 and CaM-SRC3 interaction are dependent on Ca^{2+} *in vitro*. In agreement, neural activities increased CaM-SRC3 interaction and CaM acetylation in an NMDAR-dependent way.

SRC3 belongs to the SRC family of p160 proteins, which also include SRC1 and SRC2. The SRC family proteins physically interact with steroid receptors in a ligand-dependent manner (27–29). SRC1 and SRC2 are widely expressed in several brain regions such as the cortex, hippocampus, amygdala, cerebellum, and hypothalamus (30, 31). By contrast, SRC3 is expressed predominantly in the hippocampus and very sparsely in the hypothalamus (20, 30). Different from SRC1 and SRC2, which are mainly distributed in the nucleus, SRC3 is highly expressed in the cytoplasm of mouse brain, which suggests that SRC3 could regulate both genomic and non-genomic signaling pathways of steroid hormones.

SRC3 has been extensively studied in the fields of cancer, metabolism, and endocrinology (20, 32–35). However, the function of SRC3 in the brain remains largely unknown. An early study showed that female but not male *Src3* mutant mice increased anxiety in the open field test (36). A previous study indicated that SRC3 regulates dendritic arborization in cultured hippocampal neurons (37). Here we demonstrate that SRC3 is important for synaptic plasticity in the hippocampus and contextual fear memory. The LTP at SC-CA1 synapses in the hippocampus is linked with contextual fear memory (25, 26). However, other brain regions such as amygdala and the hippocampal-amygdala circuit are also important for contextual fear memory (38–41). Injecting SI-2 into the brain ventricle may affect both the hippocampus and amygdala (or other brain regions important for contextual fear memory) and thus has significant effects on behaviors.

The PTP at SC-CA1 synapses was also significantly reduced after inhibition or knockdown of SRC3, which indicated that SRC3 was important for LTP induction. This hypothesis is supported by the finding that SRC3 inhibitor SI-2 attenuates LTP when applied before but not after the induction of LTP. Considering that acetylation of CaM is increased within 1 min after cLTP stimulation in hippocampal slices (15), it is reasonable that acetylation of CaM is also involved in the induction of LTP. Together, these results indicate that both SRC3 and CaM acetylation are important for LTP induction.

SRC3 has an RID and HAT domain. The RID of SRC3 contains three LXXLL (in which X represents any amino acid) motifs, which form amphipathic α -helices and are responsible for binding with nuclear receptors (19). The KAT domain is localized in the C terminus of SRC3 and exhibits histone acetyltransferase activity (42), although its cellular substrates are incompletely identified. The previous study indicated that the presence of RID did not influence the activity of KAT domain of SRC3 (42). Our finding that SRC3 acetylates CaM and contributes to CaMKII α activation and synaptic plasticity will broaden our understanding of SRC3 function in the brain. The CaM deacetylase is currently unknown and waits for future investigation. Given that CaM is a ubiquitous Ca^{2+} sensor and has multiple target proteins (43), future work is warranted to study whether SRC3-mediated CaM acetylation could regulate Ca^{2+} signaling in other tissues in addition to the brain.

Experimental procedures

Animals

C57BL/6N male mice at age of 7–8 weeks were used in experiments unless otherwise described. Animals were housed in rooms at 23 °C and 50% humidity in a 12 h light/dark cycle and with food and water available ad libitum. All experimental procedures were approved by the Institutional Animal Care and Use Committees of East China Normal University. Rosa26-Cas9 knockin mice were generated by Shanghai Model Organisms Center, Inc. The knockin mice used in this study were all males.

Subcellular fractions

Mouse brain tissues were homogenized in Buffer A (0.32 M sucrose, 1 mM $MgCl_2$, 1 mM PMSF, and a protease inhibitor cocktail). Homogenates were passed through a filter to remove cell debris and centrifuged at 500g for 5 min in a fixed angle rotor to yield P1 and S1 fractions. P1 fractions were washed in Buffer B containing 10 mM KCl, 1.5 mM $MgCl_2$, 10 mM Tris-HCl (pH 7.4) and centrifuged at 500g for 5 min. Pellets were dissolved in Buffer C containing 20 mM HEPES (pH 7.9), 25% glycerol, 1.5 mM $MgCl_2$, 1.4 M KCl, 0.2 mM EDTA, 0.2 mM PMSF, 0.5 mM DTT and incubated on a shaker at 4 °C for 30 min. After centrifugation at 12,000g for 10 min, the supernatant of P1 was collected as nuclear proteins. The S1 fraction was centrifuged at 10,000g for 10 min to yield P2 that contains membranes and synaptosomes and the cytoplasmic S2.

Western blot

Nuclear and S2 solutions were mixed with 6 \times SDS-PAGE sample buffer. P2 fractions were directly dissolved in 1 \times SDS-PAGE sample buffer. Respective subcellular fractions were resolved on SDS-PAGE and transferred to nitrocellulose membranes, which were incubated in the TBS buffer containing 0.1% Tween-20 and 5% milk for 1 h at room temperature before incubation with a primary antibody overnight at 4 °C. After wash, the membranes were incubated with an

HRP-conjugated secondary antibody in the same TBS buffer for 1 h at room temperature. Immunoreactive bands were visualized by ChemiDoc™ XRS + Imaging System (BIO-RAD) using enhanced chemiluminescence (Pierce) and analyzed with Image J (NIH). The primary antibodies used were as follows: anti-SYN1, Cell Signaling (2312); anti-HAT1, Abcam (ab194296); anti-P300, Santa Cruz (sc-585); anti-CBP, Cell Signaling (7389); anti-PCAF, Cell Signaling (3378); anti-GCN5, Cell Signaling (3305); anti-TIP60, Abcam (ab23886); anti-ELP3, Abcam (ab190907); anti-SRC3, Cell Signaling (5765); anti-SRC2, Bioss (bs-20558R); anti-SRC1, Bioss (bs-10603R); anti- α -tubulin, Cell Signaling (3873); anti-Histone H3, Cell Signaling (9715); anti-Flag, Sigma (F7425); anti-CaM, Millipore (05-173); anti-CaMKII α , Cell Signaling (11945); anti-p-CaMKII α Thr²⁸⁶, Sigma (SAB4300228); anti-Acetyllysine, Cell Signaling (9441); anti-p-GluR1 Ser⁸³¹, Abcam (ab109464); anti-GluR1, Abcam (ab109450); anti-GST, Abmart (12G8), and anti-His, Abmart (10E2). The site-specific anti-Ac-CaM antibodies were generated in house (15).

Cell transfection

The HEK293 cells were transfected with different KAT plasmids using linear PEI (Polysciences, 23966-2). The KAT plasmids we used were all Flag-tagged. The constructs of P300, PCAF, and GCN5 were from addgene. The plasmids of TIP60 and SRC3 were kindly provided by Dr Jiemin Wong (ECNU, China). The pan KDAC inhibitor TSA is from Sigma (T1952) and was used as a positive control to analyze CaM acetylation.

In vitro acetylation assay

Acetylation was assayed as previously described (44) with modification. In brief, precipitated Flag-SRC3 from HEK293 cells or His-tagged SRC3 KAT domain purified from bacteria, 0.5 mM acetyl-CoA (Sigma), and 1 μ g GST-tagged WT or 3KR-CaM were incubated for 30 min at 31 °C in acetylation buffer (50 mM HEPES, pH 8.0, 10% glycerol, 1 mM DTT, 1 mM PMSF, 0.1 mM CaCl₂, 1 μ M TSA, and 2.5 mM NAM) with constant shaking. Reactions were stopped by an addition of 2 \times SDS sampling buffer, followed by western blot with anti-acetyllysine antibodies (Cell signaling, 9441) or site-specific anti-Ac-CaM antibodies generated in house. The purified GST-tagged CBP KAT domain is from Sigma (SRP 5173).

GST pull-down

GST-WT, 3KR and His-WT, acetylated CaM were expressed in *Escherichia coli* BL21 cells and purified using Glutathione Sepharose 4 Fast Flow (GE Health) according to the manufacturer's instructions. His-tagged SRC3 HAT domain or acetylated CaM proteins were purified using Ni-NTA agarose beads (QIAGEN) following the manufacturer's protocols. For binding assays, eluted His-SRC3-KAT was incubated with immobilized GST-CaM for 2 h at 4 °C with 1 mM EGTA (no Ca²⁺, as a negative control), 0.01 mM, or 0.1 mM CaCl₂. The mixture was then washed, eluted, and subjected to western blot with anti-His and anti-GST antibodies (Abmart). To determine the K_d value, His-SRC3-KAT

was incubated with immobilized GST-CaM for 2 h at 4 °C with different concentrations of Ca²⁺. The mixture was then washed, eluted, and subjected to ELISA assay with anti-His antibodies and HRP-conjugated goat-anti-mouse secondary antibodies. The calcium concentration was adjusted to 0, 0.1, 0.3, 1, 3, 10, 30, 100 μ M using the calcium calibration buffer kit (Invitrogen, C-3008MP). A Ca²⁺ titration curve was used to calculate K_d value by nonlinear regression analysis.

Coimmunoprecipitation

Lysates of hippocampal slices containing 500 μ g protein were diluted in RIPA buffer without Triton X-100 or EGTA and incubated with rabbit SRC3 antibodies (Cell Signaling, 5765) immobilized on Protein A/G PLUS-Agarose (Santa Cruz) overnight at 4 °C. Immunoprecipitated proteins were subjected to western blot and probed with mouse anti-CaM antibodies (Millipore, 05-173). SRC3 was immunoprecipitated with α -Flag M2 agarose (Sigma, A2220) from HEK293 cells overexpressing pCMV-Flag-SRC3 following the manufacturer's protocols. The immunoprecipitated proteins were subjected to western blot and probed with mouse anti-CaM antibodies (Millipore, 05-173).

Chemical LTP

cLTP stimulation in hippocampal slices was performed as previously described (45). Briefly, cLTP was induced by incubating slices for 15 min in aCSF lacking MgCl₂ and containing 4 mM CaCl₂, 100 μ M picrotoxin, 50 μ M forskolin, and 100 nM rolipram. Slices were transferred to a well containing standard aCSF solution.

Electrophysiology

Hippocampal slices from 7–8-week-old mice were placed in a recording chamber continuously superfused with prewarmed (32 \pm 1 °C) aCSF at a rate of 3 ml/min. fEPSPs were evoked (0.033 Hz, 0.1 ms current pulses) in the CA1 stratum radiatum by stimulating Schaffer collateral (SC) with a two-concentric bipolar stimulating electrode (FHC) and recorded in current-clamp by a HEKA EPC 10 (HEKA Elektronik) amplifier with aCSF-filled glass pipettes (1–5 M Ω). fEPSPs were evoked by a serial of incremental intensities (0.01–0.2 mA in 0.01 mA increments, 100 μ s in duration, at 0.033 Hz) to build up an I/O curve. For PPF, two stimuli were delivered and separated by 20 ms, 50 ms, 100 ms, 150 ms, and 200 ms. LTP was induced using three trains of theta burst stimulation (10 bursts at 5 Hz, each having 50 pulses, at 100 Hz) with intertrain intervals of 30 s.

We took use of voltage clamp to record whole cell LTP as previously described (46). Three-week-old male mice were used for whole cell LTP recording with 20 μ M BIC in the aCSF. Briefly, EPSCs of hippocampal CA1 pyramidal neurons were evoked (0.1 Hz, 0.1 ms current pulses) by stimulating SC with electrode placed 200 μ m away from recorded neurons at –70 mV. LTP was induced by three trains of HFS (100 Hz, 1 s) separated by 20 s with the patched cells depolarized to –20 mV. To avoid “wash-out” of LTP, the HFS

was applied within 10 min after achieving whole cell configuration.

All data were acquired at a 10 kHz sampling rate of using PATCHMASTER version 2 x 90.1 software (HEKA Elektronik) and filtered offline at 2 kHz. Analysis was performed with Neuromatic version 3.0 (<http://www.neuromatic.thinkrandom.com>). Each EPSP or EPSC trace was normalized to baseline. Two consecutive EPSP or six consecutive EPSC traces were averaged to generate 1-min bin, which generated LTP summary time course graphs. For the LTP of field potential, the magnitude of LTP was calculated at an average of normalized EPSP amplitudes 50–60 min after TBS. For whole-cell LTP, the magnitude of LTP was calculated at the averaged of normalized EPSC amplitudes 45–50 min after HFS.

Generation of adenoassociated virus (AAV) and lentivirus (LV)

To screen *Src3* gRNA sequences and avoid potential off-target effects, we used the Cas9 design tool (<http://crispr.mit.edu>). The *Src3* gRNA 1# and 2# were designed to target exon 1 and 2 of mouse *Src3* gene, respectively. The target sequence for *Src3* gRNA 1# and 2# were atccgctggccgctgagtctcgg and acagtggtgagaagtggcgacgg, respectively. The pAAV-U6-*Src3* gRNA (1#) v2.0-U6-*Src3* gRNA (2#) v2.0-CMV-EGFP cDNA was cloned into the pAAV-MCS vector, which was packaged into AAV2/9 chimeric virus with AAV9 capsids and AAV2 ITR (inverted terminal repeat) element. To generate AAV that expresses WT and 3KR-CaM, we first subcloned cDNA of WT or 3KR-CaM into the pAAV-Syn1 promoter-EGFP-p2A-MCS-3Flag vector before packaging the AAV.

The lentivirus vectors expressing *Cam* shRNA and shRNA-resistant *Cam* genes were kindly provided by Dr Thomas C. Südhof (47). We changed the sequence of IRES in the original vector to p2A to increase the expression level of EGFP. We also mutated the WT-CaM to 3 KR or 3KQ-CaM in the lentivirus vector. All the AAV and lentivirus were generated in OBiO Technology Corp, Ltd.

Stereotaxic injection

For virus injection, Rosa26-Cas9 knockin mice at age of 7–8 weeks were anesthetized with 1% pentobarbital sodium (100 mg/kg, i.p.) and were placed in a stereotaxic apparatus (RWD Life Science). Viruses were injected bilaterally in the CA1 regions of hippocampus with the coordinates: anteroposterior (AP) –2.7 mm, mediolateral (ML) \pm 2.25 mm, dorsoventral (DV) –1.625 mm relative to bregma. Each injection used 0.5 μ l AAV or 1 μ l LV and took 5 and 10 min for AAV and LV, respectively. After injection, the glass pipette was left in place for 5 min in order to facilitate diffusion of the virus. The injection sites were examined at the end of the experiments, and animals with incorrect injection site were excluded from the data analysis. Three weeks after AAV injection or 2 weeks after LV injection, mice were subjected to experiments. All surgery was conducted with aseptic technique.

Administration of SI-2 into lateral ventricles

A permanent cannula was placed in the right lateral ventricle with the coordinates: AP –0.58 mm, ML +1.20 mm, DL –1.20 mm relative to bregma. Animals at age of 9–10 weeks were allowed to recover from surgery for a week before experiments. The infusion cannula was connected *via* PE20 tubing to a microsyringe driven by a microinfusion pump (KDS 310, KD Scientific). The SRC3 inhibitor SI-2 (TOCRIS, 5964) was prepared in aCSF (0.5 M) and 1 μ l stocking solution was injected into the right lateral ventricle through infusion cannula. The half-life of SI-2 is 12 h (22). The injection sites were examined at the end of the experiments, and animals with incorrect injection site were excluded from the data analysis.

Contextual fear conditioning

The investigators who performed behavioral analysis were blind to the treatment of the mice. Mice at age of 10–11 weeks were first habituated to the behavioral room and apparatus (Fear Conditioning System, Panlab) for 5 min. During training, mice were placed in the conditioning chamber and exposed to three foot shocks (2 s, 0.5 mA) with an interval of 30 s. One day after training, mice were returned to the same chamber where training was performed to evaluate contextual fear learning. SI-2 was delivered 1 h before training or 1 h before test. Freezing during training and testing was scored using PACKWIN software. Data were expressed as percent freezing in 180-s epochs, with each epoch divided into 12 bins.

Statistical analysis

All the data were shown as mean \pm SD. Comparisons between two groups were made using two-tailed *t* test. Comparisons between three or more groups were made using one-way ANOVA analysis followed by Tukey's post-hoc test. Data on the open field and contextual fear learning were analyzed by two-way-ANOVA. Statistically significant difference was indicated as follows: ****p* < 0.001, ***p* < 0.01, and **p* < 0.05. The statistical analysis was performed with the software of GraphPad Prism 8.

Data availability

All data supporting the results presented herein are available from the article paper.

Acknowledgments—This work was supported by grants from National Natural Science of China (No. 31970900), the Fundamental Research Funds for the Central Universities, the Program for Professor of Special Appointment (Eastern Scholar) at Shanghai Institutions of Higher Learning. We thank Dr Jiemin Wong (ECNU, China) for providing the TIP60 and SRC3 constructs.

Author contributions—H.-L. Z. and D.-M. Y. conceptualization; H.-L. Z., W. H., B. Z. and D.-M. Y. data curation; D.-M. Y. funding acquisition; H.-L. Z., W. H., Y.-Q. D, B. Z., and P. Y. investigation; H.-L. Z. methodology; D.-M. Y. project administration; D.-M. Y. supervision; H.-L. Z. validation; H.-L. Z.

visualization; H.-L. Z. writing-original draft; D.-M. Y. writing-review and editing.

Conflict of interest—The authors declare that they have no conflicts of interest with the contents of this article.

Abbreviations—The abbreviations used are: AAV, adenoassociated virus; CaM, calmodulin; CaMKII α , calcium/calmodulin-dependent protein kinase II α ; Co-IP, coimmunoprecipitated; KAT, lysine acetyltransferase; KDAC, lysine deacetyltransferase; LTP, long-term potentiation; LV, lentivirus; PPF, paired-pulse facilitation; PTP, posttetanic potentiation; RID, receptor-interaction domain; SRC3, steroid receptor coactivator 3.

References

- Flavell, S. W., and Greenberg, M. E. (2008) Signaling mechanisms linking neuronal activity to gene expression and plasticity of the nervous system. *Annu. Rev. Neurosci.* **31**, 563–590
- Ma, H., Groth, R. D., Cohen, S. M., Emery, J. F., Li, B., Hoedt, E., Zhang, G., Neubert, T. A., and Tsien, R. W. (2014) gammaCaMKII shuttles Ca(2+)(+)/CaM to the nucleus to trigger CREB phosphorylation and gene expression. *Cell* **159**, 281–294
- Coba, M. P. (2019) Regulatory mechanisms in postsynaptic phosphorylation networks. *Curr. Opin. Struct. Biol.* **54**, 86–94
- Soderling, T. R., and Derkach, V. A. (2000) Postsynaptic protein phosphorylation and LTP. *Trends Neurosci.* **23**, 75–80
- Allfrey, V. G., Faulkner, R., and Mirsky, A. E. (1964) Acetylation and Methylation of histones and their possible role in the regulation of RNA Synthesis. *Proc. Natl. Acad. Sci. U. S. A.* **51**, 786–794
- Alarcon, J. M., Malleret, G., Touzani, K., Vronskaya, S., Ishii, S., Kandel, E. R., and Barco, A. (2004) Chromatin acetylation, memory, and LTP are impaired in CBP \pm mice: A model for the cognitive deficit in Rubinstein-Taybi syndrome and its amelioration. *Neuron* **42**, 947–959
- Guan, J. S., Haggarty, S. J., Giacometti, E., Dannenberg, J. H., Joseph, N., Gao, J., Nieland, T. J., Zhou, Y., Wang, X., Mazitschek, R., Bradner, J. E., DePinho, R. A., Jaenisch, R., and Tsai, L. H. (2009) HDAC2 negatively regulates memory formation and synaptic plasticity. *Nature* **459**, 55–60
- Vecsey, C. G., Hawk, J. D., Lattal, K. M., Stein, J. M., Fabian, S. A., Attner, M. A., Cabrera, S. M., McDonough, C. B., Brindle, P. K., Abel, T., and Wood, M. A. (2007) Histone deacetylase inhibitors enhance memory and synaptic plasticity via CREB:CBP-dependent transcriptional activation. *J. Neurosci.* **27**, 6128–6140
- Hsieh, J., and Gage, F. H. (2005) Chromatin remodeling in neural development and plasticity. *Curr. Opin. Cell Biol.* **17**, 664–671
- Xia, Z., and Storm, D. R. (2005) The role of calmodulin as a signal integrator for synaptic plasticity. *Nat. Rev. Neurosci.* **6**, 267–276
- Malenka, R. C., and Bear, M. F. (2004) LTP and LTD: An embarrassment of riches. *Neuron* **44**, 5–21
- Lisman, J., Yasuda, R., and Raghavachari, S. (2012) Mechanisms of CaMKII action in long-term potentiation. *Nat. Rev. Neurosci.* **13**, 169–182
- Swaminathan, P. D., Purohit, A., Hund, T. J., and Anderson, M. E. (2012) Calmodulin-dependent protein kinase II: Linking heart failure and arrhythmias. *Circ. Res.* **110**, 1661–1677
- Parra, V., and Rothermel, B. A. (2017) Calcineurin signaling in the heart: The importance of time and place. *J. Mol. Cell Cardiol.* **103**, 121–136
- Zhang, H. L., Zhao, B., Han, W., Sun, Y. B., Yang, P., Chen, Y., Ni, D., Zhang, J., and Yin, D. M. (2021) Acetylation of calmodulin regulates synaptic plasticity and fear learning. *J. Biol. Chem.* <https://doi.org/10.1016/j.jbc.2021.101034>
- Allis, C. D., Berger, S. L., Cote, J., Dent, S., Jenuwien, T., Kouzarides, T., Pillus, L., Reinberg, D., Shi, Y., Shiekhattar, R., Shilatifard, A., Workman, J., and Zhang, Y. (2007) New nomenclature for chromatin-modifying enzymes. *Cell* **131**, 633–636
- Sebti, S., Prebois, C., Perez-Gracia, E., Bauvy, C., Desmots, F., Pirot, N., Gongora, C., Bach, A. S., Hubberstey, A. V., Palissot, V., Berchem, G., Codogno, P., Linares, L. K., Liaudet-Coopman, E., and Pattingre, S. (2014) BAT3 modulates p300-dependent acetylation of p53 and autophagy-related protein 7 (ATG7) during autophagy. *Proc. Natl. Acad. Sci. U. S. A.* **111**, 4115–4120
- Yoshida, M., Kijima, M., Akita, M., and Beppu, T. (1990) Potent and specific inhibition of mammalian histone deacetylase both *in vivo* and *in vitro* by trichostatin A. *J. Biol. Chem.* **265**, 17174–17179
- Xu, J., Wu, R. C., and O'Malley, B. W. (2009) Normal and cancer-related functions of the p160 steroid receptor co-activator (SRC) family. *Nat. Rev. Cancer* **9**, 615–630
- Xu, J., Liao, L., Ning, G., Yoshida-Komiya, H., Deng, C., and O'Malley, B. W. (2000) The steroid receptor coactivator SRC-3 (p/CIP/RAC3/AIB1/ACTR/TRAM-1) is required for normal growth, puberty, female reproductive function, and mammary gland development. *Proc. Natl. Acad. Sci. U. S. A.* **97**, 6379–6384
- Patton, B. L., Molloy, S. S., and Kennedy, M. B. (1993) Autophosphorylation of type II CaM kinase in hippocampal neurons: Localization of phospho- and dephosphokinase with complementary phosphorylation site-specific antibodies. *Mol. Biol. Cell* **4**, 159–172
- Song, X., Chen, J., Zhao, M., Zhang, C., Yu, Y., Lonard, D. M., Chow, D. C., Palzkill, T., Xu, J., O'Malley, B. W., and Wang, J. (2016) Development of potent small-molecule inhibitors to drug the undruggable steroid receptor coactivator-3. *Proc. Natl. Acad. Sci. U. S. A.* **113**, 4970–4975
- Mammen, A. L., Kameyama, K., Roche, K. W., and Haganir, R. L. (1997) Phosphorylation of the alpha-amino-3-hydroxy-5-methylisoxazole4-propionic acid receptor GluR1 subunit by calcium/calmodulin-dependent kinase II. *J. Biol. Chem.* **272**, 32528–32533
- Barria, A., Muller, D., Derkach, V., Griffith, L. C., and Soderling, T. R. (1997) Regulatory phosphorylation of AMPA-type glutamate receptors by CaM-KII during long-term potentiation. *Science* **276**, 2042–2045
- Takemoto, K., Iwanari, H., Tada, H., Suyama, K., Sano, A., Nagai, T., Hamakubo, T., and Takahashi, T. (2017) Optical inactivation of synaptic AMPA receptors erases fear memory. *Nat. Biotechnol.* **35**, 38–47
- Penn, A. C., Zhang, C. L., Georges, F., Royer, L., Breillat, C., Hossy, E., Petersen, J. D., Humeau, Y., and Choquet, D. (2017) Hippocampal LTP and contextual learning require surface diffusion of AMPA receptors. *Nature* **549**, 384–388
- Chen, X., Liu, Z., and Xu, J. (2010) The cooperative function of nuclear receptor coactivator 1 (NCOA1) and NCOA3 in placental development and embryo survival. *Mol. Endocrinol.* **24**, 1917–1934
- Zhou, H. J., Yan, J., Luo, W., Ayala, G., Lin, S. H., Erdem, H., Ittmann, M., Tsai, S. Y., and Tsai, M. J. (2005) SRC-3 is required for prostate cancer cell proliferation and survival. *Cancer Res.* **65**, 7976–7983
- Zhou, X. E., Suino-Powell, K. M., Li, J., He, Y., Mackeigan, J. P., Melcher, K., Yong, E. L., and Xu, H. E. (2010) Identification of SRC3/AIB1 as a preferred coactivator for hormone-activated androgen receptor. *J. Biol. Chem.* **285**, 9161–9171
- Nishihara, E., Yoshida-Komiya, H., Chan, C. S., Liao, L., Davis, R. L., O'Malley, B. W., and Xu, J. (2003) SRC-1 null mice exhibit moderate motor dysfunction and delayed development of cerebellar Purkinje cells. *J. Neurosci.* **23**, 213–222
- Yore, M. A., Im, D., Webb, L. K., Zhao, Y., Chadwick, J. G., Jr., Molenda-Figueira, H. A., Haidacher, S. J., Denner, L., and Tetel, M. J. (2010) Steroid receptor coactivator-2 expression in brain and physical associations with steroid receptors. *Neuroscience* **169**, 1017–1028
- Louie, M. C., Zou, J. X., Rabinovich, A., and Chen, H. W. (2004) ACTR/AIB1 functions as an E2F1 coactivator to promote breast cancer cell proliferation and antiestrogen resistance. *Mol. Cell Biol.* **24**, 5157–5171
- Liu, Z., Liao, L., Zhou, S., and Xu, J. (2008) Generation and validation of a mouse line with a floxed SRC-3/AIB1 allele for conditional knockout. *Int. J. Biol. Sci.* **4**, 202–207
- Wu, Z., Yang, M., Liu, H., Guo, H., Wang, Y., Cheng, H., and Chen, L. (2012) Role of nuclear receptor coactivator 3 (Nco3) in pluripotency maintenance. *J. Biol. Chem.* **287**, 38295–38304

EDITORS' PICK: SRC3 as a CaM acetyltransferase

35. Chen, W., Lu, X., Chen, Y., Li, M., Mo, P., Tong, Z., Wang, W., Wan, W., Su, G., Xu, J., and Yu, C. (2017) Steroid receptor coactivator 3 contributes to host defense against Enteric bacteria by recruiting neutrophils via upregulation of CXCL2 expression. *J. Immunol.* **198**, 1606–1615
36. Stashi, E., Wang, L., Mani, S. K., York, B., and O'Malley, B. W. (2013) Research resource: Loss of the steroid receptor coactivators confers neurobehavioral consequences. *Mol. Endocrinol.* **27**, 1776–1787
37. Storchel, P. H., Thummler, J., Siegel, G., Aksoy-Aksel, A., Zampa, F., Sumer, S., and Schratz, G. (2015) A large-scale functional screen identifies Noxa1 and Ncoa3 as regulators of neuronal miRNA function. *EMBO J.* **34**, 2237–2254
38. Maren, S., Phan, K. L., and Liberzon, I. (2013) The contextual brain: Implications for fear conditioning, extinction and psychopathology. *Nat. Rev. Neurosci.* **14**, 417–428
39. Tovote, P., Fadok, J. P., and Luthi, A. (2015) Neuronal circuits for fear and anxiety. *Nat. Rev. Neurosci.* **16**, 317–331
40. Kim, W. B., and Cho, J. H. (2017) Encoding of discriminative fear memory by input-specific LTP in the amygdala. *Neuron* **95**, 1129–1146.e1125
41. Kim, W. B., and Cho, J. H. (2020) Encoding of contextual fear memory in hippocampal-amygdala circuit. *Nat. Commun.* **11**, 1382
42. Chen, H., Lin, R. J., Schiltz, R. L., Chakravarti, D., Nash, A., Nagy, L., Privalsky, M. L., Nakatani, Y., and Evans, R. M. (1997) Nuclear receptor coactivator ACTR is a novel histone acetyltransferase and forms a multimeric activation complex with P/CAF and CBP/p300. *Cell* **90**, 569–580
43. Chin, D., and Means, A. R. (2000) Calmodulin: A prototypical calcium sensor. *Trends Cell Biol.* **10**, 322–328
44. Min, S. W., Cho, S. H., Zhou, Y., Schroeder, S., Haroutunian, V., Seeley, W. W., Huang, E. J., Shen, Y., Masliah, E., Mukherjee, C., Meyers, D., Cole, P. A., Ott, M., and Gan, L. (2010) Acetylation of tau inhibits its degradation and contributes to tauopathy. *Neuron* **67**, 953–966
45. Otmakhov, N., Khibnik, L., Otmakhova, N., Carpenter, S., Riahi, S., Asrican, B., and Lisman, J. (2004) Forskolin-induced LTP in the CA1 hippocampal region is NMDA receptor dependent. *J. Neurophysiol.* **91**, 1955–1962
46. Wu, D., Bacaj, T., Morishita, W., Goswami, D., Arendt, K. L., Xu, W., Chen, L., Malenka, R. C., and Sudhof, T. C. (2017) Postsynaptic synaptotagmins mediate AMPA receptor exocytosis during LTP. *Nature* **544**, 316–321
47. Pang, Z. P., Cao, P., Xu, W., and Sudhof, T. C. (2010) Calmodulin controls synaptic strength via presynaptic activation of calmodulin kinase II. *J. Neurosci.* **30**, 4132–4142



Hai-Long Zhang is a postdoctoral fellow in the Institute of Neuroscience at Soochow University, after getting the PhD degree at East China Normal University. He studies the function and regulation of protein acetylation in synaptic plasticity and memory. He demonstrated that acetylation of CaM, a ubiquitous Ca^{2+} sensor, was critical for synaptic plasticity and contextual fear memory; he also identified SRC3 as the most active KAT responsible for CaM acetylation.